JOURNAL OF GUIDANCE, CONTROL, AND DYNAMICS
Vol. 18, No. 4, July–August 1995

Consistent Model Reduction of Experimental Modal Parameters for Reduced-Order Control

K. F. Alvin,* L. D. Peterson,† and K. C. Park‡
University of Colorado, Boulder, Colorado 80309

The problem of synthesizing reduced-order linear models of vibrating structures for the design of fixed-order dynamic feedback control is investigated. The present technique builds on a recently developed procedure for constructing an objective set of mass and stiffness matrices from measured modal parameters that are akin to the Craig–Bampton synthesized matrices obtained from finite element models (FEMs). The constructed mass and stiffness matrices are determined directly from the identification of experimental data, however, rather than through correlation or reconciliation of a FEM. A model truncation criterion is then applied to the identified minimum-order mass and stiffness model to satisfy certain observability/controllability requirements for the reduced model. Numerical examples illustrate the effectiveness of the proposed technique for synthesizing reduced-order controllers from system realizations of experimental data. The dynamic performance of the resulting closed-loop models is assessed using the known full-order structural dynamics and compared with existing model reduction techniques.

I. Introduction

IT is well established that the stability and performance of model-based controllers for large space structures (LSSs) is highly dependent on the accuracy of the dynamic model used for control design. Unfortunately, the accuracy of analytical models [e.g., finite element models (FEMs)] formulated from design drawings of structures are necessarily limited by the governing assumptions of linear behavior, the statistical variance in the properties of structural components due to fabrication tolerances, and the increased heterogeneity of the structures being modeled. It is generally acknowledged that even a high degree of modeling precision cannot compensate for a lack of experience with the real measured behavior of complex structures. For this reason, system identification of experimental data has played an important role in the synthesis of model-based dynamic compensation.

Unfortunately, whereas highly accurate minimal-order realizations of experimental data may be obtained for model-based controller synthesis, the resulting model order may still be quite large. Thus, the designer must frequently truncate either the system realization or the controller dimension, compromising accuracy so that the size of the resulting design is small enough for computationally feasible real-time control. This is the well-known problem of model reduction for control. Figure 1 illustrates the possible design procedures for synthesizing reduced-order model (ROM) controllers for systems possessing larger order dynamics.

The focus of this paper is on methods of reducing the identified model of the system being controlled such that the resultant controller design is feasible for real-time implementation. Typically, identified models of experimental data are truncated by either eliminating the normal modes of the model that are less critical to performance or isolated from the control bandwidth, or by eliminating model states that are the least controllable or observable. If the model states are the normal modal displacements and velocities, this is termed a modal truncation and requires a measure of the modal controllability and observability.[1] Otherwise, it is possible to transform to an equivalent realization in which the controllability and observability grammians for the state definition are equal and diagonal. This is referred to as a balanced realization, and truncation of the least controllable/observable states is then termed a balanced reduction.[2] In fact, the realization determined by the basic Eigenvalue Realization Algorithm (ERA) identification procedure[3] leads to a balanced model, and the selection of the identified model order for experimental data effectively leads to a balanced reduction of the measured dynamics.

In FEM-based structural dynamics, a widely accepted procedure for substructure model synthesis and reduction is the so-called Craig–Bampton (CB) component mode synthesis method.[4] A CB model is a reduction of the second-order mass and stiffness of the FEM with respect to a selected set of physical (usually boundary) degrees of freedom (DOF). The CB representation of mass and stiffness is constructed for a larger order model through a full set of constraint modes and a selected set of fixed-interface normal modes. An important characteristic of the CB representation is that, due to the inclusion of the constraint modes, the resultant model is statically complete with respect to the retained physical DOF. Here, a statically complete model is one that retains all component modes necessary to exactly capture the static, or zero-frequency, response of the full-order system. For free-free systems, this implies that the rigid-body modes are exactly preserved.

In recent years, a number of researchers have noted the advantages of static completeness and the CB representation in model reductions for control. Blelloch and Carney[5] noted the advantages of static completeness for preserving closed-loop poles and transfer func-

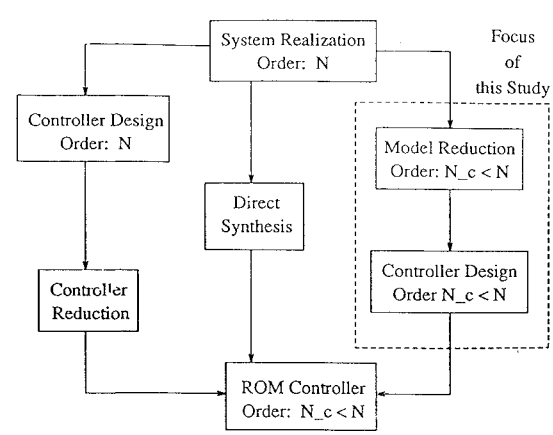

Fig. 1 Fixed-order controller design paths.

Received Nov. 15, 1993; revision received July 29, 1994; accepted for publication Aug. 31, 1994.

*Research Associate, Department of Aerospace Engineering Sciences and Center for Space Structures and Controls. Member AIAA.

†Assistant Professor, Department of Aerospace Engineering Sciences and Center for Space Structures and Controls. Senior Member AIAA.

‡Professor, Department of Aerospace Engineering Sciences and Center for Space Structures and Controls. Associate Fellow AIAA.

tions in a model reduction procedure. Craig and Hale[6] have shown that a block-Krylov vector space spanned by the fixed-interface modes is controllable (observable) when formed recursively from the constraint modes. Recently, Triller and Kammer[7] have directly addressed controllability/observability measures for the CB fixed-interface modes, their advantages over normal-mode measures, and application to the problem of model reduction for controller design.

This paper presents a new physical model-based reduction technique for measured modal parameters in reduced-order control. To this end, we demonstrate a minimal-order mass and stiffness representation of the model[8] that is used in conjunction with physical variable-based reduction methods as an alternative to modal truncation or balanced reduction. An important advantage of this approach is that it does not require correlation of a large-order FEM of the structure. Instead, the minimum-order stiffness and mass matrices are directly constructed from the modal parameters and then treated as if they were CB representations of mass and stiffness determined from a FEM. Another advantage of the present technique is that we can utilize the physically based model reduction of the CB model, which preserves the full static completeness of the identified model. In summary, the present technique directly synthesizes reduced-order statically complete models from system identifications while bypassing the complications of correlating larger order FEMs.

The remainer of the paper is organized as follows. In Sec. II, the system realization process and methods for extracting modal parameters from system realizations are briefly reviewed. In Sec. III, a recently developed procedure for representing modal data in a mass-stiffness form similar to the CB synthesis technique for FEMs is detailed. The resultant mass and stiffness matrices have an asymptotic equivalence to the Guyan-reduced and CB-synthesized matrices as the full modal spectrum is identified. Section IV details the reduction of the identified minimum-order mass and stiffness model through truncation of the fixed-interface modal coordinates characteristic of the CB representation. In Sec.V, the reduced model basis is evaluated through numerical examples and compared to truncation of normal vibration modes and balanced model states. Finally, conclusions are presented in Sec.VI.

II. System Identification and Normal-Mode Parameters

In modern modal testing, the system identification typically begins by obtaining frequency-domain transfer functions over the bandwidth of interest for each input-output pairing through discrete Fourier transforms and ensemble averaging. Modal parameters are determined either by curve-fitting techniques or from an equivalent system realization of the data in the time or frequency domain. The ERA[3] and the Polyreference technique[9] are two such methods that have become widely available and utilized for structural dynamic systems. The ERA is designed to systematically determine a minimum-order discrete-time model to approximate the system pulse response. The algorithm uses numerical techniques that are robust in the presence of repeated roots and measurement noise. The discrete-time model can be converted to a corresponding set of continuous-time equations, viz.,

$$\begin{aligned} \dot{x}(t) &= Ax(t) + Bu(t) \\ y(t) &= Cx(t) + Du(t) \end{aligned} \tag{1}$$

Efficient implementations of the ERA and its relationship to other system realization algorithms are detailed in Refs. 10 and 11. The extraction of the damped modes and complex mode shapes from the general system realization form (1) is briefly reviewed in Ref. 3.

In Ref. 12, a general transformation-based algorithm has been developed that consistently extracts the modal parameters of second-order dynamics from the general state-space equations (1). The common basis-normalized structural identification (CBSI) procedure obtains the correct normal (i.e., undamped) modal properties when the system damping is exactly proportional and a particular approximation in the more general damping case by a similarity transformation of the state-space model (1) to the normal-mode form of the associated second-order equations of motion. Mass orthonormalization of the eigenvectors is determined through driving-point measurements (i.e., collocated actuator and sensor).

III. Construction of Minimal-Order Mass and Stiffness Matrices

One area of recent interest in structural identification has been the determination of mass and stiffness matrices directly from system realizations of experimental data.[13] Many such direct solutions suffer, however, from the limitation that the number of identified modes and the number of modal sensors be equal. The present minimal-order mass and stiffness procedure bypasses this limitation by enriching the physical model with the complete set of measured modes, independent of the number of sensors. This allows the resulting model to express contributions of all the modes observable from the available sensors. We now review a method for constructing reduced-order and minimal-order mass and stiffness matrices directly from measured normal modal parameters that have asymptotic equivalence to existing FEM reduction and synthesis methods.

A. Component Mode Reduction of Finite Element Models

Component mode synthesis (CMS) techniques are generally applied to FEMs to both reduce the problem order and synthesize subsystem models into global models through interface compatibility conditions. In the present discussion, we are interested only in the use of component modes to accurately and efficiently reduce the order of a single-system model.

In one of the most widely known and applied component mode techniques, the so-called CB method,[4] the component modes utilized are the full set of constraint modes augmented by a truncated set of fixed-interface modes. The constraint modes and fixed-interface modes are always defined with respect to a set of physical DOF q_m. The complement of q_m is defined as q_i such that the full set of physical DOF q is given by

$$q = \begin{Bmatrix} q_m \\ q_i \end{Bmatrix} \tag{2}$$

and the equations of motion are written as

$$\mathcal{M}\ddot{q} + \mathcal{D}\dot{q} + \mathcal{K}q = f \tag{3}$$

where $\mathcal{M}$, $\mathcal{D}$, and $\mathcal{K}$ are the system mass, viscous damping, and stiffness matrices, respectively, and f is a vector of external forces. The eigenproblem corresponding to Eq. (3) is given as

$$\begin{gathered} \mathcal{K}\Phi_n = \mathcal{M}\Phi_n\Omega \\ \Phi_n^T\mathcal{M}\Phi_n = I \qquad \Phi_n^T\mathcal{D}\Phi = \Xi \qquad \Phi_n^T\mathcal{K}\Phi_n = \Omega \end{gathered} \tag{4}$$

where Φ_n are the mass-normalized real mode shapes, Ω is the diagonal matrix of eigenvalues equivalent to the squares of the undamped natural frequencies, and Ξ is the modal viscous damping matrix.

If we partition Eq. (3) into a measured set q_m and unmeasured (or internal) set q_i, we have

$$\begin{bmatrix} \mathcal{M}_{mm} & \mathcal{M}_{mi} \\ \mathcal{M}_{mi}^T & \mathcal{M}_{ii} \end{bmatrix} \begin{Bmatrix} \ddot{q}_m \\ \ddot{q}_i \end{Bmatrix} + \begin{bmatrix} \mathcal{D}_{mm} & \mathcal{D}_{mi} \\ \mathcal{D}_{mi}^T & \mathcal{D}_{ii} \end{bmatrix} \begin{Bmatrix} \dot{q}_m \\ \dot{q}_i \end{Bmatrix}$$

$$+ \begin{bmatrix} \mathcal{K}_{mm} & \mathcal{K}_{mi} \\ \mathcal{K}_{mi}^T & \mathcal{K}_{ii} \end{bmatrix} \begin{Bmatrix} q_m \\ q_i \end{Bmatrix} = \begin{bmatrix} f_m \\ f_i \end{bmatrix} \tag{5}$$

The constraint modes are then defined as the static displacement vectors of q corresponding to orthogonal unit displacements of q_m. Solving Eq. (5) with forces applied only to the measured DOF (i.e., $f_i = 0$), we determine that

$$q(t) = \begin{bmatrix} I \\ -\mathcal{K}_{ii}^{-1}\mathcal{K}_{mi}^T \end{bmatrix} q_m(t) = \Phi_c q_m(t) \tag{6}$$

The importance of the constraint modes Φ_c are that the static system response can be exactly expressed solely in terms of these modes for any applied force f_m. Applying Eq. (6) to $\mathcal{K}$, $\mathcal{D}$, and $\mathcal{M}$, the so-called Guyan reduced stiffness, damping, and mass[14] are

$$\begin{gathered} \bar{\mathcal{K}} = \Phi_c^T\mathcal{K}\Phi_c = \mathcal{K}_{mm} - \mathcal{K}_{mi}\mathcal{K}_{ii}^{-1}\mathcal{K}_{mi}^T \\ \bar{\mathcal{D}} = \Phi_c^T\mathcal{D}\Phi_c \qquad \bar{\mathcal{M}} = \Phi_c^T\mathcal{M}\Phi_c \end{gathered} \tag{7}$$

The resultant model no longer possesses the large-order dynamics of $\mathcal{K}$ and $\mathcal{M}$ but preserves the general behavior of the larger eigenproblem for the lowest frequency modes and modes that are strongly influenced by the retained degrees of freedom.

The Craig–Bampton CMS method can be viewed as an extension or augmentation of the statically condensed mass and stiffness of the Guyan reduction. Recalling Eq. (6), in the CB method q is represented as

$$q = \begin{bmatrix} I & 0 \\ -\mathcal{K}_{ii}^{-1}\mathcal{K}_{mi}^T & T_\xi \end{bmatrix} \begin{Bmatrix} q_m \\ \xi \end{Bmatrix} = T \begin{Bmatrix} q_m \\ \xi \end{Bmatrix} \tag{8}$$

where ξ are the augmented generalized DOF and T_ξ are the displacements of q_i with respect to unit displacements of ξ. Applying this to $\mathcal{K}$ gives

$$\hat{\mathcal{K}} = T^T \mathcal{K} T = \begin{bmatrix} \bar{\mathcal{K}} & 0 \\ 0 & T_\xi^T \mathcal{K}_{ii} T_\xi \end{bmatrix} \tag{9}$$

Thus, $\hat{\mathcal{K}}$ is block diagonal, composed of the Guyan reduced stiffness matrix and a residual symmetric stiffness matrix. Note that we have not yet defined ξ as fixed-interface modal coordinates of set i; the form of $\hat{\mathcal{K}}$ is a consequence of Eq. (8), which defines ξ as a subspace orthogonal to q_m through $\mathcal{K}$. To uniquely define ξ, it is specified that T_ξ are the mass-orthonormalized eigenvectors of the generalized eigenproblem

$$\begin{gathered} \mathcal{K}_{ii} T_\xi = \mathcal{M}_{ii} T_\xi \Omega_\xi \\ T_\xi^T \mathcal{K}_{ii} T_\xi = \Omega_\xi \qquad T_\xi^T \mathcal{M}_{ii} T_\xi = I \end{gathered} \tag{10}$$

Using Eq. (10) to fully define T_ξ, the CB stiffness and mass matrices are given by

$$\begin{aligned} \hat{\mathcal{K}} &= T^T \mathcal{K} T = \begin{bmatrix} \bar{\mathcal{K}} & 0 \\ 0 & \Omega_\xi \end{bmatrix} \\ \hat{\mathcal{M}} &= T^T \mathcal{M} T = \begin{bmatrix} \bar{\mathcal{M}} & \mathcal{M}_c \\ \mathcal{M}_c^T & I \end{bmatrix} \end{aligned} \tag{11}$$

where

$$\mathcal{M}_c = \mathcal{M}_{mi} T_\xi - \mathcal{K}_{mi} \mathcal{K}_{ii}^{-1} \mathcal{M}_{ii} T_\xi \tag{12}$$

is a mass coupling between q_m and ξ and $\bar{\mathcal{M}}$ is the Guyan-reduced mass given by Eq. (7).

B. Minimal-Order Experimental Mass and Stiffness

Alternative representations of the Guyan reduction and CB models can be found in terms of the normal modes of the full-order system. We begin by assuming that the measured modes from test completely span the dynamics such that the model representation in modal coordinates is a completely equivalent realization. Comparing partitions of the global flexibility matrix (i.e., inverse of the stiffness matrix) with respect to the test-measured DOF, the Guyan-reduced stiffness matrix is found as

$$\bar{\mathcal{K}} = \left[\phi_m \Omega^{-1} \phi_m^T\right]^{-1} \tag{13}$$

where ϕ_m if the partition of the mass-normalized mode shapes Φ_n with respect to the physical q_m dispacement DOF and Ω is the diagonal matrix of the squares of the undamped natural frequencies of the corresponding modes. Similarly, we can find the Guyan-reduced mass and damping matrices as

$$\begin{aligned} \bar{\mathcal{M}} &= \bar{\mathcal{K}} \phi_m \Omega^{-2} \phi_m^T \bar{\mathcal{K}} \\ \bar{\mathcal{D}} &= \bar{\mathcal{K}} \phi_m \Omega^{-1} \Xi \Omega^{-1} \phi_m^T \bar{\mathcal{K}} \end{aligned} \tag{14}$$

The reduced system matrices given by Eqs. (13) and (14) are theoretically consistent with the Guyan reduction in the limit as the full eigenspectrum of Eq. (5) is measured. In addition, they are a function only of the partition of the mode shapes at the measured locations and thus can be directly calculated from the measured test data.

For incorporation of purely rigid-body modes, the correct reduced stiffness and mass matrices are given by

$$\begin{aligned} \bar{\mathcal{K}} &= \bar{\mathcal{K}}_f - \bar{\mathcal{K}}_f \phi_{m_r} \left(\phi_{m_r}^T \bar{\mathcal{K}}_f \phi_{m_r}\right)^{-1} \phi_{m_r}^T \bar{\mathcal{K}}_f \\ \bar{\mathcal{M}} &= \bar{\mathcal{K}} \phi_{m_f} \Omega_f^{-2} \phi_{m_f}^T \bar{\mathcal{K}} + \bar{\mathcal{K}}_f \phi_{m_r} \left(\phi_{m_r}^T \bar{\mathcal{K}}_f \phi_{m_r}\right)^{-2} \phi_{m_r}^T \bar{\mathcal{K}}_f \end{aligned} \tag{15}$$

where ϕ_{m_r} and ϕ_{m_f} are the partitions of the mass-normalized mode shapes into rigid-body and flexible modes, Ω_f is the nonzero partition of Ω corresponding to the flexible modes, and

$$\bar{\mathcal{K}}_f = \left[\phi_{m_f} \Omega_f^{-1} \phi_{m_f}^T\right]^{-1}$$

The mass matrix $\bar{\mathcal{M}}$ as calculated from Eq. (15) is not only positive definite whereas $\bar{\mathcal{K}}$ is positive semidefinite but in fact correctly preserves the mass orthonormalization of the mode shapes ϕ_{m_r}.

The determination of a minimum-order equivalent mass and stiffness from test is based on the mass and stiffness form of the Craig–Bampton CMS method. Starting from $\bar{\mathcal{K}}$, we can construct the minimal-order stiffness $\hat{\mathcal{K}}$ by augmenting the measured mode shapes ϕ_m by a vector basis for the residual dynamic DOF ξ. We define the dynamic residual matrix as

$$\Delta\Omega = \Omega - \phi_m^T \bar{\mathcal{K}} \phi_m = \Omega - \phi_m^T \left(\phi_m \Omega^{-1} \phi_m^T\right)^{-1} \phi_m \tag{16}$$

The required minimal rank augmentation of q_m is determined through a singular-value decomposition of the dynamic residual matrix $\Delta\Omega$, viz.,

$$PSP^T = \text{svd}(\Delta\Omega)$$

Examination of the singular values indicates the dimension of the augmented coordinates ξ,

$$\Delta\Omega = PSP^T = P_p S_p P_p^T \tag{17}$$

Having determined a basis P_p for the augmented coordinates, we now augment ϕ_m by the rows of P_p^T that span the singular values and solve the inverse problem:

$$\begin{aligned} \begin{bmatrix} \bar{\mathcal{K}} & 0 \\ 0 & \mathcal{K}_{\text{res}} \end{bmatrix} &= \begin{bmatrix} \phi_m \\ P_p^T \end{bmatrix}^{-T} \Omega \begin{bmatrix} \phi_m \\ P_p^T \end{bmatrix}^{-1} \\ \begin{bmatrix} \bar{\mathcal{M}} & \bar{\mathcal{M}}_c \\ \bar{\mathcal{M}}_c^T & \mathcal{M}_{\text{res}} \end{bmatrix} &= \left[\begin{bmatrix} \phi_m \\ P_p^T \end{bmatrix} \begin{bmatrix} \phi_m^T & P_p \end{bmatrix} \right]^{-1} \end{aligned} \tag{18}$$

Finally, the augmented DOF are orthonormalized for consistency with the definition of ξ in Eq. (9) by solving the generalized eigenproblem:

$$\begin{gathered} \mathcal{K}_{\text{res}} U = \mathcal{M}_{\text{res}} U \Omega_\xi \\ U^T \mathcal{K}_{\text{res}} U = \Omega_\xi \qquad U^T \mathcal{M}_{\text{res}} U = I \end{gathered} \tag{19}$$

and performing a final transformation on the mass and stiffness matrices:

$$\begin{aligned} \hat{\mathcal{K}} &= \begin{bmatrix} \bar{\mathcal{K}} & 0 \\ 0 & U^T \mathcal{K}_{\text{res}} U \end{bmatrix} = \begin{bmatrix} \bar{\mathcal{K}} & 0 \\ 0 & \Omega_\xi \end{bmatrix} \\ \hat{\mathcal{M}} &= \begin{bmatrix} \bar{\mathcal{M}} & \bar{\mathcal{M}}_c U \\ U^T \bar{\mathcal{M}}_c^T & U^T \mathcal{M}_{\text{res}} U \end{bmatrix} = \begin{bmatrix} \bar{\mathcal{M}} & \mathcal{M}_c \\ \mathcal{M}_c^T & I \end{bmatrix} \end{aligned} \tag{20}$$

The primary experimental design requirement for determining the equivalent minimal-order mass and stiffness matrices is measurement of a collocated sensor at the driving point of the structure. This sensor allows for the experimental mode shapes to be mass normalized on the basis of the force input and structural response data. Further details of this method are given in Ref. 8. In the next section, we utilize the minimal-order mass and stiffness representation of the measured modal parameters to facilitate a structural model reduction for active control.

IV. Reduction of Minimal-Order Mass and Stiffness Models

We now examine the use of minimum-order mass and stiffness models for the design of fixed-order controllers. As reviewed in Sec. III, this model form is not only similar to a CB representation of an equivalent FEM of the system, but is in fact asymptotically equivalent to the CB model in the limit as the full modal spectrum of the CB model is identified. That is, given all the modes of a CB model of a structure and the corresponding mode shapes at the physical boundary DOF retained in the CB representation, the CB mass and stiffness matrices can be reconstructed exactly for the contributions of the constraint modes and all fixed interface modes that are controllable/observable from the boundary DOF.

Therefore, we can apply existing controllability and observability measures for the CB representation to our minimum-order measured mass and stiffness models. We now review Triller and Kammer's recent work,[7] which established an equivalence between the mass coupling matrix $\mathcal{M}_c$ and fixed-interface mode controllability.

A. Effective Interface Mass and Controllability

Let us write the undamped equations of motion for Eq. (2) in terms of the CB (or equivalently the measured minimum-order) mass and stiffness matrices, viz.,

$$\begin{bmatrix} \bar{\mathcal{M}} & \mathcal{M}_c \\ \mathcal{M}_c^T & I \end{bmatrix} \begin{Bmatrix} \ddot{q}_m \\ \ddot{\xi}_r \end{Bmatrix} + \begin{bmatrix} \bar{\mathcal{K}} & 0 \\ 0 & \Omega_r \end{bmatrix} \begin{Bmatrix} q_m \\ \xi_r \end{Bmatrix} = \begin{bmatrix} I \\ 0 \end{bmatrix} u \tag{21}$$

where it is assumed that the retained physical DOF q_m are exactly those DOF at which the control forces u are applied. The equations of motion for the fixed interface (or equivalently residual) modal variables ξ_r are then given as

$$\ddot{\xi}_r + \Omega_r \xi_r = -\mathcal{M}_c^T \ddot{q}_m \tag{22}$$

Therefore, $-\mathcal{M}_c^T$ is effectively a modal participation factor matrix for the accelerations $\ddot{q}_m$ that excite the fixed-interface modes. From this concept, a measure termed the effective interface mass can be defined for each fixed-interface modal coordinate ξ_{ri}, viz.,

$$\Sigma_i = \frac{\sum_{j=1}^{n_u} \mathcal{M}_c(j,i)^2}{\mathcal{M}_c \mathcal{M}_c^T} \tag{23}$$

where n_u is the dimension of the vector q_m.

Ignoring eigenvalue multiplicity considerations and relative weightings of the DOF in q_m, a relative measure of controllability of fixed-interface coordinate ξ_{ri} with respect to input accelerations at the interface DOF q_m is directly given by its effective interface mass measure Σ_i. Using this same measure as the relative controllability with respect to the input forcing function u ignores the relative stiffness and mass properties that couple the q_m DOF but does give an efficient approximate ordering of the fixed-interface modes.

B. Procedure for Model Reduction

The procedure for reducing the minimum-order mass and stiffness model is straightforward. First, we retain the DOF corresponding to the actuators and also possibly some or all noncollocated sensor DOF. The model reduction then amounts to selection of the residual modal coordinates ξ_{ri}, whose controllability can be ranked through the effective interface mass measure Σ_i. That is, if the total controller order is to be limited to N_C and the order of the second-order physical (i.e., mass and stiffness) variables q_m is n_u, then the number of retained residual modal coordinates ξ_{ri} is equal to

$$n_r = \tfrac{1}{2} N_C - n_u \tag{24}$$

Generally, the n_r coordinates ξ_{ri} with the largest effective interface mass Σ_i will be retained.

In addition, further reduction in the order of the state estimator is possible because, by retaining the physical measurement DOF, it is not necessary to estimate the variables that are effectively direct measurements. If n_z measurement DOF from the variables q_m are treated in this fashion and thus not estimated, the number of retained coordinates ξ_{ri} is increased to

$$n_r = \tfrac{1}{2} N_C - n_u + n_z \tag{25}$$

There may still be reason to include the direct measurement DOF in the ROM estimator, for example, to filter the measurement signal noise. In the example problems to follow, we will include the DOF q_m in the estimator states for conservatism and for consistency in performance comparisons with other ROM controllers based on normal modal truncation and internal balanced reduction.

We summarize the reduction of system realizations based on minimum-order mass and stiffness as follows:

Step 1: Identify experimental data in the general state-space form (1) using the ERA or equivalent methods.

Step 2: Transform Eq. (1) using CBSI or other methods to extract the identified mass-normalized modal parameters ϕ_m, Ω, and Ξ.

Step 3: Apply the minimum-order mass and stiffness method detailed in Sec. III to compute the reduced stiffness $\bar{\mathcal{K}}$ and minimum-order mass and stiffness $\hat{\mathcal{M}}$ and $\hat{\mathcal{K}}$. The same transformations can be applied to the modal damping matrix Ξ to compute an equivalent physical damping matrix $\hat{\mathcal{D}}$ that is consistent with $\hat{\mathcal{M}}$ and $\hat{\mathcal{K}}$.

Step 4: Compute the effective interface mass measures Σ_i for the residual dynamics using the $\mathcal{M}_c$ partition of $\hat{\mathcal{M}}$. Truncate the residual partitions of $\hat{\mathcal{K}}$ and $\hat{\mathcal{M}}$ with the smallest Σ_i until the desired controller order is attained. The resultant ROM is of a second-order mass-damping-stiffness form, which is easily recast in state-space form for use in modern control design algorithms.

V. Implementation and Evaluation

A numerical example of a planar truss structure was formulated for performance evaluation of the proposed model reduction technique. Figure 2 illustrates the structural layout highlighting the physical locations of the inputs and outputs. The bold arrows symbolize the force inputs with collocated velocity outputs. In addition there are three additional velocity outputs that are noncollocated for a total of six possible measurements and three applied feedback control forces. The model was formulated using only truss elements and translational DOF for a total of 36 physical DOF.

A. Determination of Minimal-Order Mass and Stiffness

We begin with the system identification of simulated experimental data. In order to model both the effects of measurement noise and some degree of nonlinearity or nonrepeatability in the structural response, a normal distribution of 5% rms noise was added to the simulated impulse responses. The system damping was assumed to be proportional, with 0.1% modal damping ratios for the 36 structural modes. The impulse response for the 18 transfer functions was identified using a form of the ERA method, as implemented in Ref. 10. CBSI was then used to extract the normal modal parameters, and the minimum-order mass and stiffness subsequently obtained. The reduced stiffness was computed for a range of system realization model orders and the convergence of the norm of the six reduced stiffness matrices was studied to verify the required realization accuracy. This convergence is shown in Fig. 3. From this, the identified state-space realization was estimated at 70 or equivalently 35 modes. Figures 4 and 5 illustrate the resultant minimum-order stiffness and mass matrices, respectively, in which the residual modes have been ordered by the residual frequency magnitude. Observe that the magnitude of the elements of the off-diagonal mass coupling submatrix $\mathcal{M}_c$ in Fig. 5 is largest for the lowest residual modal coordinates.

B. Controllability, Static Completeness, and Reduction

As outlined in Sec. IV, the effective interface mass measure can be quickly computed from the mass coupling matrix $\mathcal{M}_c$ for each of the residual modal coordinates. To compare and contrast the minimum-order mass and stiffness (MOMS) reduction method to existing techniques, we have selected reduction based on normal-mode truncation and reduction via balanced-state truncation[2] as two alternative candidate techniques. A balanced-state model is one for which each of the internal states are equally controllable and observable, and the controllability and observability grammians are

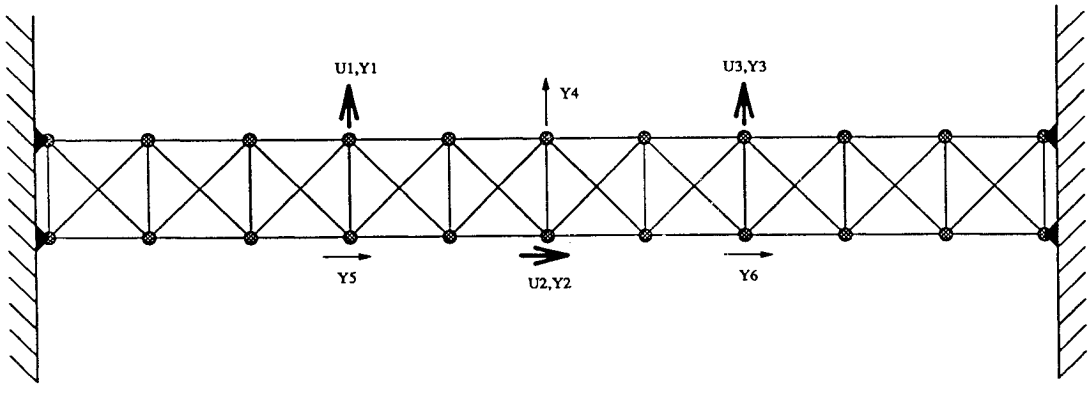

Fig. 2 Thirty-six DOF planar truss example problem.

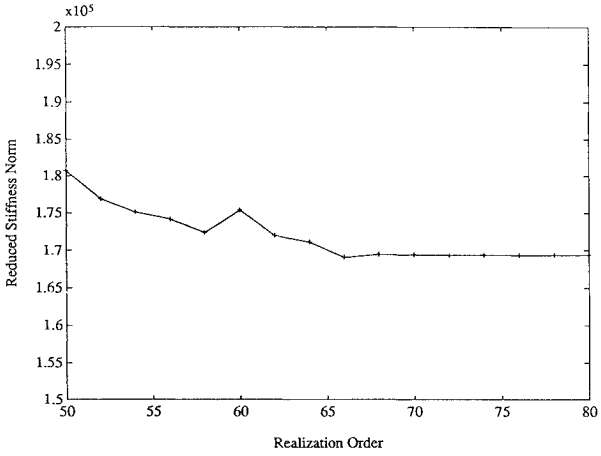

Fig. 3 Convergence of reduced stiffness matrix.

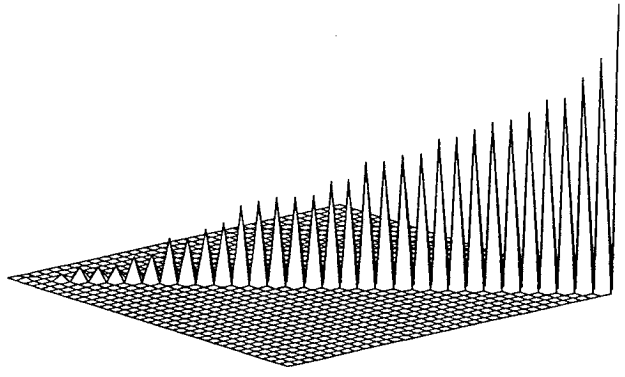

Fig. 4 Identified minimum-order stiffness matrix.

diagonal. For normal-mode truncation, we have selected two candidate controllability measures for evaluation.

Modal Truncation: Modal Singular Value (MT-MSV)

Here we order the identified normal modes by a measure of their contribution to the discrete measured responses used in the system identification. The measure chosen is the modal singular value,[15] which is roughly analogous to the product of the discrete-time controllability and observability.

Modal Truncation: Mode Shape Magnitude (MT-MSM)

A gross comparative measure of controllability can be obtained from the mass-normalized mode shapes by computing the norm of the partition of each mode shape at the control input locations. That is, letting ϕ_u^T be the normal modal participation factors of the input u,

$$\phi_{ui}^T = \Phi_{ni}^T \hat{B} \tag{26}$$

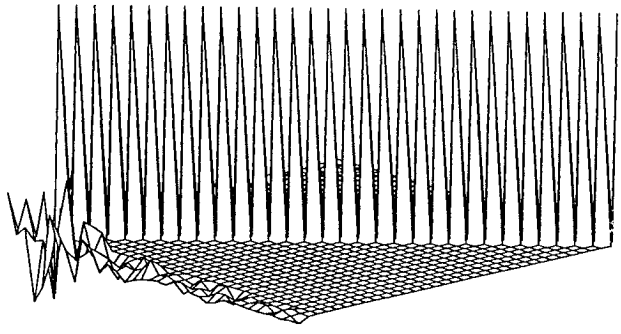

Fig. 5 Identified minimum-order mass matrix.

the relative controllability of normal mode i could be given by

$$\gamma = \phi_{ui}^T \phi_{ui} \tag{27}$$

This measure is not entirely appropriate, however, in that it favors modes with higher acceleration response rather than zero-frequency displacement gain. Therefore, we replace Eq. (27) with

$$\gamma = \frac{\phi_{ui}^T \phi_{ui}}{\omega_{ni}^2} \tag{28}$$

which favors modes contributing more significantly to the static behavior of the system.

For this numerical example, two orders of model reduction were studied; $N_C = 24$ and $N_C = 12$, given that the maximum model order identified from the system realization was $N = 70$. The reduced-order model states were selected independent of the selected measurements since the MOMS and MT-MSM reductions are based solely on controllability measures. For the balanced and MT-MSV reductions, which are also dependent on observability, the full set of six possible measurements were utilized.

In Table 1, the ordered modal controllability measures, normalized to a maximum of 1.00, are presented for the residual modes of the MOMS method, and for the two normal modal truncation criteria, up to $N_C = 30$. The balanced reduction is not included here because it is not based upon modal controllability measures. In Table 2, a measure of the error in static completeness of each model is given. This error measure is computed as the percentage difference in the norm of the system receptance, viz.,

$$\lim_{\omega \to 0} \mathcal{H}_d(\omega) = \lim_{\omega \to 0} C_d(i\omega I - A)^{-1} B = -C_d A^{-1} B \tag{29}$$

Note that the MOMS model is indeed equivalent to the full-order identified model in terms of its static behavior. The small error present is a result of the system identification of the data with 5% rms noise, which results in a small variance between the identified model and the exact dynamics. Note also that the static completeness errors of the balanced reduction and modal truncation ordering are also fairly small, though not as good as the MOMS model.

Table 1 Modal controllability measures

Second-order ROM DOF	MOMS		MT-MSV		MT-MSM	
	Residual mode	Normalized measure	Normal mode	Normalized measure	Normal mode	Normalized measure
1	N/A	N/A	1	1.0000	1	1.0000
2	N/A	N/A	2	0.8514	2	0.1512
3	N/A	N/A	3	0.5379	3	0.0774
4	1	1.0000	7	0.5116	14	0.0372
5	4	0.7410	4	0.4607	7	0.0183
6	3	0.4497	18	0.4423	6	0.0146
7	2	0.4384	12	0.3501	5	0.0071
8	6	0.3269	11	0.3437	12	0.0068
9	7	0.1080	5	0.3301	13	0.0062
10	8	0.0441	16	0.3280	11	0.0060
11	10	0.0367	26	0.3257	18	0.0053
12	14	0.0321	20	0.3246	9	0.0049
13	12	0.0305	8	0.3086	16	0.0046
14	9	0.0253	13	0.2959	20	0.0043
15	18	0.0206	17	0.2863	10	0.0042

Table 2 Error in ROM static completeness

Model	N_c	Percent error
Full order	70	0.0499
MOMS	24	0.0499
	12	0.0499
MT-MSV	24	1.8439
	12	2.7921
Balanced Reduction	24	2.2376
	12	4.2887
MT-MSM	24	1.6722
	12	3.0317

C. Linear Quadratic Regulator/Gaussian Design and Evaluation Procedure

To objectively compare and contrast the performance of each ROM controller, a systematic optimal linear quadratic regulator/Gaussian (LQR/LQG) compensation design procedure was followed. The exact full-order system is given as

$$\begin{aligned} \dot{x} &= Ax + Bu + Hw \\ y &= Cx \qquad z = Mx + v \end{aligned} \tag{30}$$

where w are system force disturbances, z are the feedback measurements, v is the measurement noise, H is the disturbance state influence array, and M is the state measurement influence array. The noise characteristics are assumed to be white with Gaussian distribution. The identified reduced-order model is then given as

$$\begin{aligned} \dot{x}_R &= A_R x_R + B_R u + H_R w \\ y &= C_R x_R \qquad z = M_R x_R + v \end{aligned} \tag{31}$$

Utilizing the separation principle,[16] the regulator gain G and the estimator gain K may be separately determined. For the regulator, a full-state feedback law $u = Gx_R$ was obtained by minimizing the performance index

$$J = \int_0^\infty \left(\frac{1}{2} y^T Q y + \frac{\rho^2}{2} u^T R u \right) dt \tag{32}$$

where

$$Q = 0.250 \times I \qquad R = 0.010 \times I \tag{33}$$

and ρ is a parameter to be varied so that the controller performance may be examined over a range of possible designs. For the estimator, a standard LQG design was obtained using disturbances w at the control actuator locations and measurement noise v, viz.,

$$\dot{\tilde{x}}_R = A_R \tilde{x}_R + B_R u + K(z - M_R \tilde{x}) \tag{34}$$

The covariances of the disturbances and noise were assumed to be

$$\begin{aligned} E[w(t)w^T(\tau)] &= W\,\delta(t-\tau) = I\,\delta(t-\tau) \\ E[v(t)v^T(\tau)] &= V\,\delta(t-\tau) = 0.010 \times I\,\delta(t-\tau) \\ E[w(t)v^T(\tau)] &= 0 \end{aligned} \tag{35}$$

The closed-loop system with full-order system dynamics and the ROM-based controller design is then given as

$$\dot{x}_C = A_C x_C + B_C w_C \qquad y_C = C_C x_C \tag{36}$$

where

$$\begin{aligned} A_C &= \begin{bmatrix} A & BG \\ KM & A_R + B_R G - K M_R \end{bmatrix} \\ B_C &= \begin{bmatrix} H & 0 \\ 0 & K \end{bmatrix} \qquad C_C = \begin{bmatrix} C & 0 \\ 0 & G \end{bmatrix} \\ x_C &= \begin{Bmatrix} x \\ \tilde{x}_R \end{Bmatrix} \qquad w_C = \begin{Bmatrix} w \\ v \end{Bmatrix} \qquad y_C = \begin{Bmatrix} y \\ u \end{Bmatrix} \end{aligned} \tag{37}$$

The covariance of the outputs y and controls u can be determined from the covariance X_C of the closed-loop state x_C. First, solve the Lyapunov equation for X_C, viz.,

$$A_C X_C + X_C A_C^T + B_C \begin{bmatrix} W & 0 \\ 0 & V \end{bmatrix} B_C^T = 0 \tag{38}$$

Then, the covariance Y of the output and U of the control are given as

$$\begin{aligned} Y &= [C \quad 0] X_C [C \quad 0]^T \\ U &= [0 \quad G] X_C [0 \quad G]^T \end{aligned} \tag{39}$$

Finally, to quantify the output magnitude and control effort in a single parameter, we utilize the trace of the output and control covariances, viz.,

$$\sigma_y = \mathrm{tr}[Y] \qquad \sigma_u = \mathrm{tr}[U] \tag{40}$$

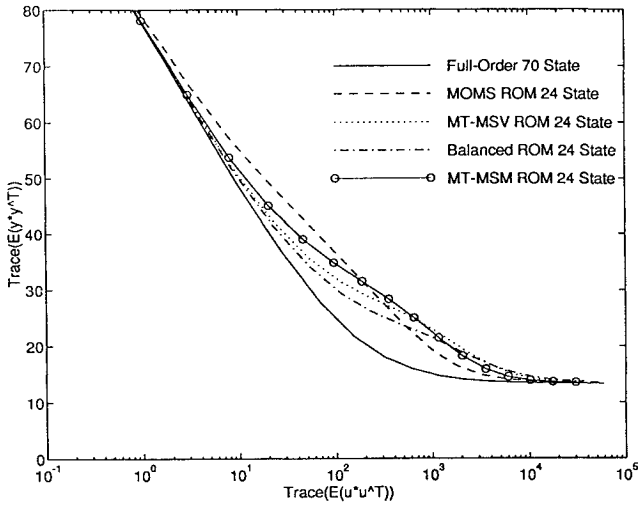

Fig. 6 Collocated feedback design: large-ROM results.

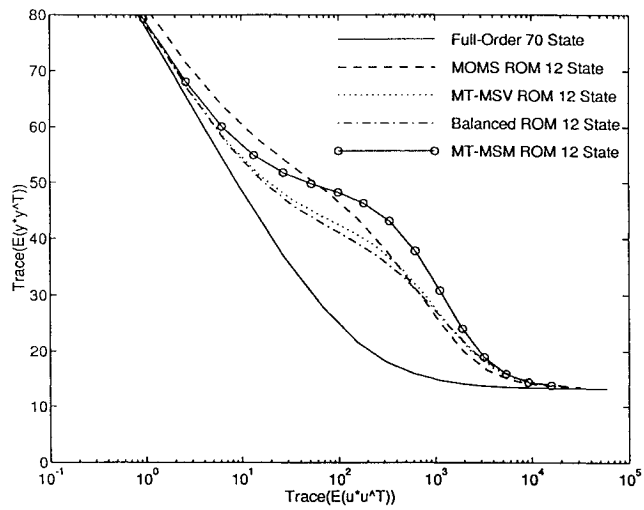

Fig. 7 Collocated feedback design: small-ROM Results.

D. Comparison of ROM Controller Performance

The controller design and evaluation procedure outlined in the preceding section was implemented for a series of system designs of the planar truss example. Each system design case consisted of a selection of measurements for feedback control and a selected reduced-order model size N_C. Figures 6 and 7 illustrate the relative ROM controller performance using the three collocated sensors for feedback. The performance is represented by plotting the trace of the output covariance Y vs the trace of the control covariance U. Relative better performance is indicated by the lower curves, since this implies higher output suppression for an equivalent control effort. The performance results reflect a variation in the performance design parameter ρ from approximately 10^{-10} up to 10^5.

The "large ROM" was limited to 24 first-order states. This corresponds to 12 vibration modes for the modal truncation ROMs and 9 residual (or fixed-interface) dynamic modes for the MOMS reduction method (plus the 3 physical measured DOF retained in the ROM). The "small ROM" was then limited to 12 first-order states, corresponding to 6 normal modes for the modal truncation ROMs and 3 residual dynamic modes for the MOMS reduction method.

From Figs. 6 and 7 it appears that the MOMS ROM controller does not outperform either the balanced reduction or the modal truncation ROM controllers except at a high control effort. It does, however, significantly outperform a modal truncation-based ROM controller where the modes have been ordered by the mass-normalized mode shape magnitude at the actuator locations as in Eq. (27). This improved performance is consistent with results of Ref. 7, which studied the relative ROM accuracy for CB model

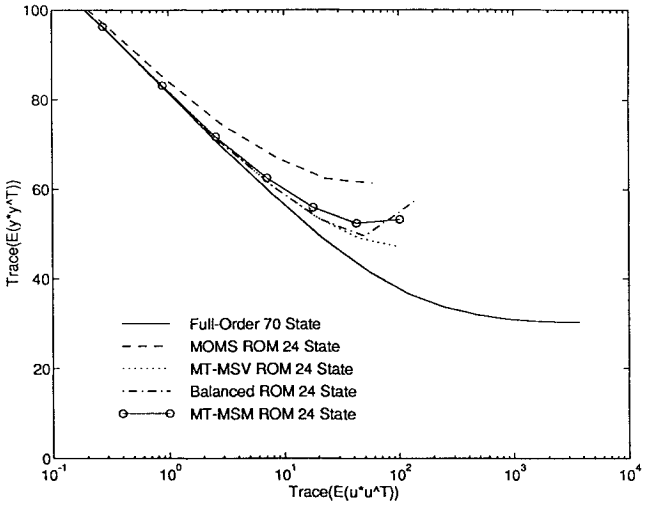

Fig. 8 Noncollocated feedback design: large-ROM results.

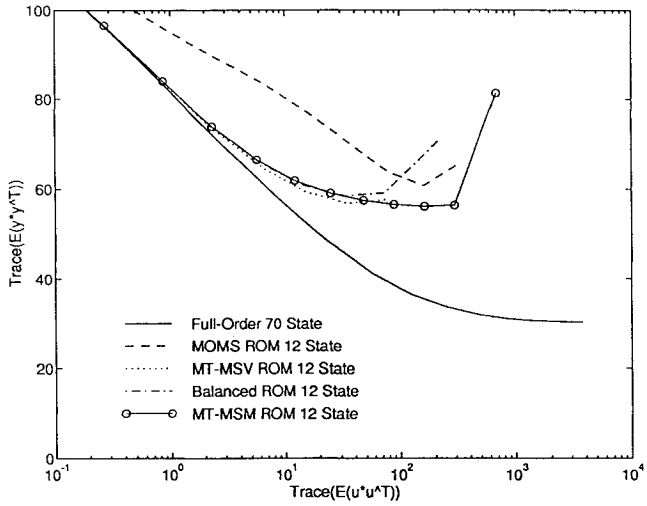

Fig. 9 Noncollocated feedback design: small-ROM results.

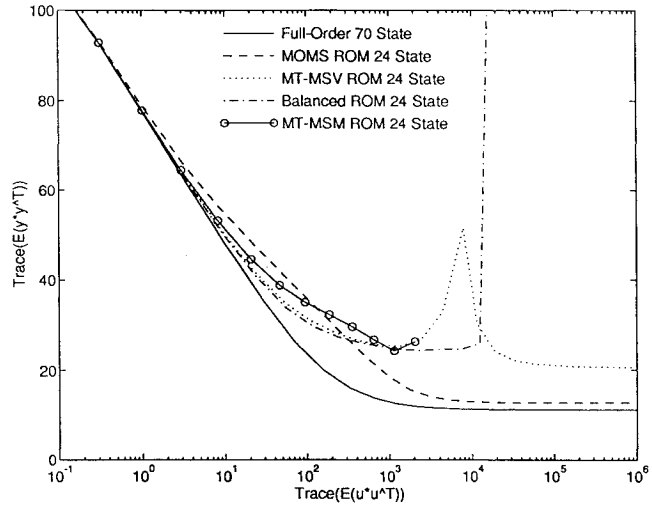

Fig. 10 Hybrid feedback design: large-ROM results.

representations vs mode shape magnitude-ordered modal truncation. For the present analysis, only modal truncation based on MSV and Eq. (28) are included for quantitative performance comparisons.

Figures 8 and 9 illustrate the relative ROM controller performance using the three noncollocated sensors for feedback. All the methods employed in the noncollocated case used the same ROM states as for the collocated case. This is because the MOMS ROM method, utilizing only actuator DOF, does not account for the noncollocated

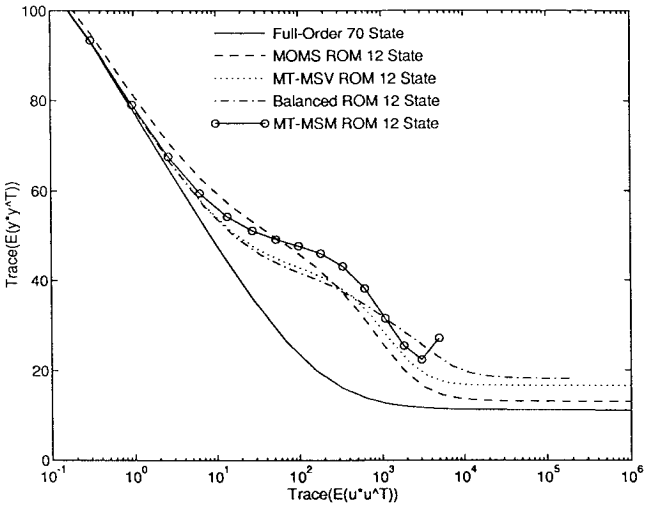

Fig. 11 Hybrid feedback design: small-ROM results.

sensor observability in the computation of the effective interface mass. As expected, this system design is much less robust as it is more dependent on the accuracy of the model. There was little appreciable difference in the stability margins of the different ROM controllers.

Finally, Figs. 10 and 11 illustrate the relative ROM controller performance using all six sensors (collocated and noncollocated) for feedback. For these hybrid cases, the MOMS ROM controllers did show a more pronounced improvement over the other ROM controllers. It is not yet clear whether this improvement was a result of the example problem being studied and the input and output locations chosen or if in fact it is due to the static completeness feature of the CB/MOMS representation.

VI. Conclusions

A new approach for reducing the order of identified structural dynamics models for active controls has been presented. The method is based on a MOMS representation of the identified normal modes, which is similar to the CB component mode synthesis representation of FEMs. The present procedure directly synthesizes the realization of experimental data and thus does not require correlation of a FEM. Model order reduction is accomplished through truncation of the residual dynamic modes of the MOMS model, which are analogous to the fixed-interface modes of CB models. The relative performance of LQR/LQG-based ROM controllers using the present procedure and existing techniques based on normal-mode truncation and balanced reduction has been detailed through numerical examples. The new reduction procedure is superior to modal truncation based on ordering the normal modes by their mass-normalized mode shape magnitudes at the actuator locations but does not outperform balanced reduction or modal truncation based on MSV and zero-frequency gain. Further work in this area should address the synthesis of ROM-based controllers from experimental data using the present procedure and implementation of those controllers for real-time active control to experimentally measure their closed-loop performance.

Acknowledgments

The work presented herein was supported under Grant NAG-1-1200 from the Control-Structure Interaction Program Office of NASA Langley Research Center and Award 959444 from Jet Propulsion Laboratory. We thank Keith Belvin of NASA Langley and John Spanos of JPL for their encouragement.

References

[1]Hughes, P. C., and Skelton, R. E., "Controllability and Observability of Linear Matrix-Second-Order Systems," *Journal of Applied Mechanics*, Vol. 47, 1980, pp. 415–420.

[2]Moore, B. C., "Principal Component Analysis in Linear Systems: Controllability, Observability, and Model Reduction," *IEEE Transactions on Automatic Control*, Vol. 26, No. 1, 1981, pp. 17–32.

[3]Juang, J. N., and Pappa, R. S., "An Eigensystem Realization Algorithm for Modal Parameter Identification and Model Reduction," *Journal of Guidance, Control, and Dynamics*, Vol. 8, No. 5, 1985, pp. 620–627.

[4]Craig, R. R., and Bampton, M. C., "Coupling of Substructures for Dynamic Analyses," *AIAA Journal*, Vol. 6, No. 7, 1968, pp. 1313–1319.

[5]Blelloch, P. A., and Carney, K. S., "Model Representations in Control/Structure Interaction," *Proceedings of the American Control Conference*, Pittsburgh, PA, 1989, pp. 2802–2807.

[6]Craig, R. R., and Hale, A. L., "Block-Krylov Component Synthesis Method for Structural Model Reduction," *Journal of Guidance, Control, and Dynamics*, Vol. 11, No. 6, 1988, pp. 562–570.

[7]Triller, M. J., and Kammer, D. C., "Controllability and Observability Measures for Craig–Bampton Substructure Representations," *Journal of Guidance, Control, and Dynamics*, Vol. 17, No. 6, 1994, pp. 1198–1204.

[8]Alvin, K. F., Peterson, L. D., and Park, K. C., "Method for Determining Minimum-Order Mass and Stiffness Matrices from Modal Test Data," *AIAA Journal*, Vol. 33, No. 1, 1995, pp. 128–135.

[9]Vold, H., Kundrat, J., Rocklin, G. T., and Russell, R., "A Multiple-Input Modal Estimation Algorithm for Mini-Computers," SAE Paper 820194; also *SAE Transactions*, Vol. 91/1, 1982, pp. 815–821.

[10]Peterson, L. D., "Efficient Computation of the Eigensystem Realization Algorithm," *Proceedings of the 10th International Modal Analysis Conference*, Feb. 1992; also *Journal of Guidance, Control, and Dynamics* (to be published).

[11]Juang, J.-N., "Mathematical Correlation of Modal Parameter Identification Methods via System Realization Theory," *International Journal of Analytical and Experimental Modal Analysis*, Vol. 2, No. 1, 1987, pp. 1–18.

[12]Alvin, K. F., and Park, K. C., "Second-Order Structural Identification Procedure via State Space-Based System Identification," *AIAA Journal*, Vol. 32, No. 2, 1994, pp. 397–406.

[13]Yang, C.-D., and Yeh, F.-B., "Identification, Reduction, and Refinement of Model Parameters by the Eigensystem Realization Algorithm," *Journal of Guidance, Control, and Dynamics*, Vol. 13, No. 6, 1990, pp. 1051–1059.

[14]Guyan, R. J., "Reduction of Stiffness and Mass Matrices," *AIAA Journal*, Vol. 3, No. 2, 1965, p. 380.

[15]Longman, R. W., Lew, J.-S., and Juang, J.-N., "Comparison of Candidate Methods to Distinguish Noise Modes from System Modes in Structural Identification," AIAA Paper 92-2518, April 1992.

[16]Skelton, R. E., *Dynamic Systems Control*, Wiley, New York, 1988.